Chapter 13

Paleoseismic Investigations on the Rock Valley Fault System

By Jeffrey A. Coe, James C. Yount, Dennis W. O'Leary, and Emily M. Taylor

Contents

Abstract

Paleoseismic investigations in trenches excavated across five faults in the Rock Valley Fault system provide evidence for at least five surface-rupturing paleoearthquakes in the past several hundred thousand years. Four of the faults, designated the northern, medial, and southern (two strands) faults, are in the central section of the Rock Valley Fault system southeast of Skull Mountain; the fifth fault, designated the Frenchman Flat Fault, is in Frenchman Flat near the east end of the fault system. All five faults strike N. 65°–80° E. and are expressed as scarps or lineaments in Quaternary deposits. In general, displacements are predominantly strike slip (left lateral) with a dip-slip component.

Five faulting events affecting one or more faults in the Rock Valley Fault system are estimated to have occurred at approximately 160, 120, 40±24, 13±4, and 2–1 ka. The late Pleistocene slip rate for the fault system is about 0.1 mm/yr. Estimated displacements and slip rates for individual faults are, for the (1) northern fault: average net displacement per event (four events), 2.9 m; slip rate, 0.07±0.04 mm/yr; (2) medial fault: average net displacement per event (three events), 2.5 m; slip rate, 0.023±0.010 mm/yr; (3) northern strand of the southern fault: average net displacement per event (three events), 0.1 m; slip rate, more than 0.001±0.001 mm/yr; (4) southern strand of the southern fault: average net displacement per event (three events), 0.1 m; slip rate, 0.002±0.0005 mm/yr; and (5) Frenchman Flat Fault: net displacement (one event), more than 1 m; slip rate, indeterminable. The largest surface-rupturing paleoearthquake (penultimate faulting event) caused a total of about 4.2 m of net displacement along the Rock Valley Fault system in central Rock Valley.

Introduction

The Rock Valley Fault system occupies most of east-northeast-trending Rock Valley, about 25 km southeast of the proposed repository site for the storage of high-level radioactive wastes at Yucca Mountain (fig. 1). The fault system is composed of multiple east-northeast trending strike- and oblique-slip faults that form distinct scarps and lineaments in surficial deposits and demonstrate a considerable history of Quaternary movement. The fault system constitutes a significant tectonic boundary within the Walker Lane (O'Leary, 2000) between Miocene volcanic rocks of the southwestern Nevada volcanic field to the

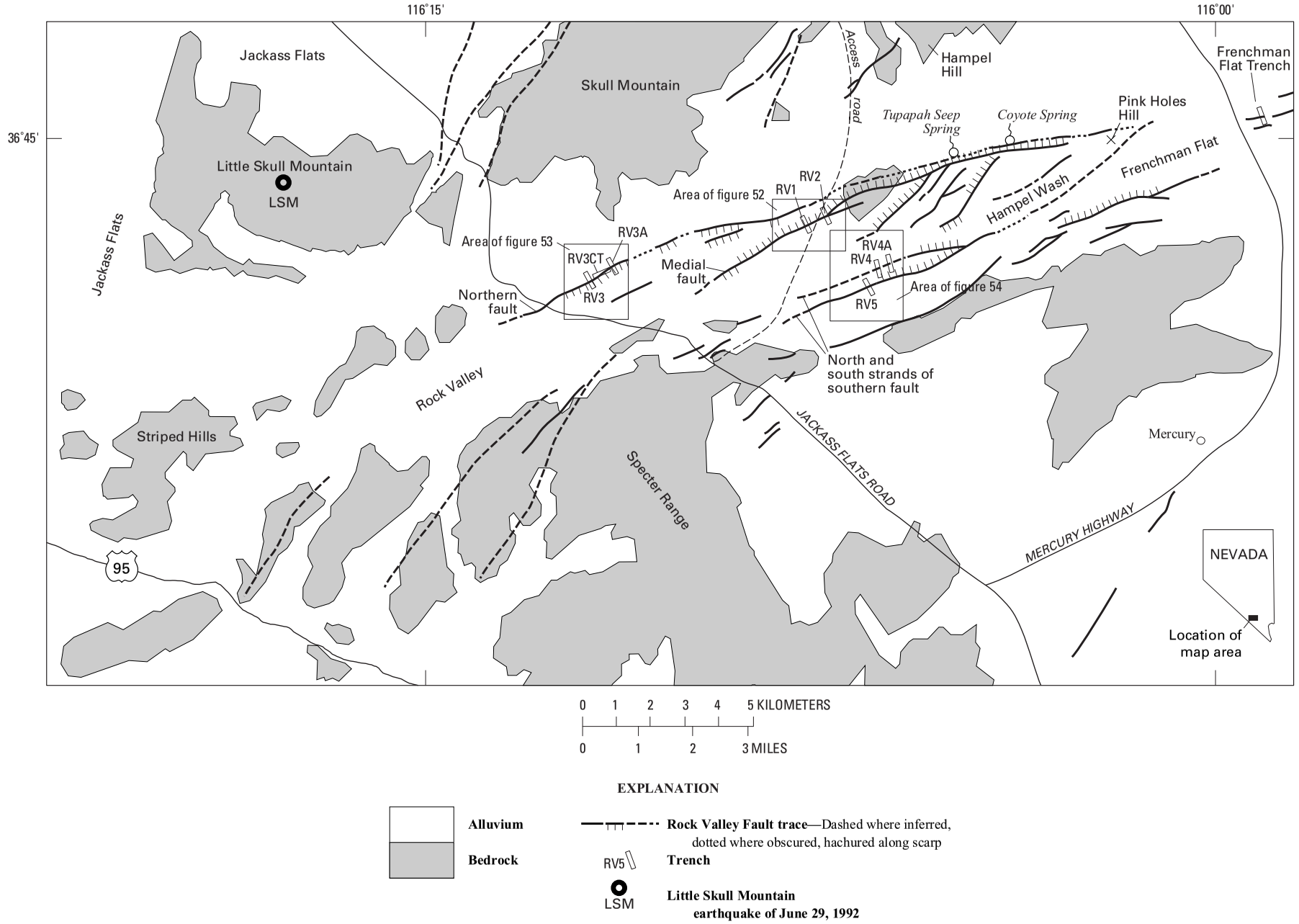

Figure 51. Geologic map of the Rock Valley area, southwestern Nevada, showing locations of trenches on the Rock Valley Fault system (figs. 1, 2).

north (Skull and Little Skull Mountains) and lower Paleozoic carbonate strata to the south (Specter Range, figs. 1, 51).

In addition to Quaternary tectonic activity, the Rock Valley Fault system has been the locus of recent, uncommonly shallow earthquakes, some of which are probably related to the aftershock sequence of the June 29, 1992, *M*=5.6 Little Skull Mountain, Nev., earthquake (Smith and Brune, 1993; Smith and others, 2000).

This chapter presents the Quaternary paleoseismic history of the Rock Valley Fault system as determined from detailed logging and interpretations of exposures in eight trenches excavated on faults along the north and south sides of the valley. Results from a previous paleoseismic investigation on a fault in central Rock Valley (Yount and others, 1987), as well as data from a trench in Frenchman Flat near the east end of the fault system, are also integrated into this summary of the paleoseismic history of the fault system.

Physiographic Setting

Rock Valley trends N. 70° E. from near U.S. Highway 95 eastward to Frenchman Flat (fig. 51), a distance of about 32 km. The valley, which gains its geographic definition from an alignment of adjacent uplands rather than by a conspicuous valley-floor depression, is primarily a tectonic rather than an erosional feature. The geomorphology of the valley floor is controlled by a network of faults (Rock Valley Fault system) that spans the length of the valley and occupies most of its width (~5 km). Frizzell and Zoback (1987) suggested that the current topographic expression of the valley probably developed after about 5 Ma. The erosion that has occurred and is presently occurring in Rock Valley is interpreted to be largely a consequence of tectonic activity—namely, differential movement (uplift or subsidence) between the east and west ends of the fault zone. A transverse drainage divide just east of the area 27 access road (fig. 51) separates the valley into an eastward-draining watershed (to Frenchman Flat by way of Hampel Wash) and a westward-draining watershed (to Amargosa Lake by way of Rock Valley Wash). The eastward-draining watershed is relatively deeply eroded; much Pleistocene alluvium has been stripped away, thus exposing the faults, the underlying Miocene rocks, and the pre-Pleistocene structural configuration of the valley floor. West of the drainage divide, the faults are expressed as lineaments or scarps in alluvium, but such features have not been observed west of long 116°15′ W. (fig. 51).

Characteristics of the Rock Valley Fault System

Three major fault sets compose the Rock Valley Fault system: (1) long, dominantly left lateral strike-slip faults that strike N. 65°–80° E.; (2) shorter normal, strike-slip or reverse relay faults, or both, that strike N. 25°–50° E.; and (3) minor normal and strike-slip faults that strike N. 10°–15° W. Three of the N. 65°–80° E.-striking faults are considered major in this study on the basis of their length, continuity, and expression in Pleistocene alluvial-fan surfaces. These faults, designated informally as the northern, medial, and southern faults (fig. 51), are composite structures that, from place to place along strike, consist of numerous subparallel planes that interlink or splay off toward the southwest. (See chap. 3 for various interpretations as to the total length of the fault system.)

The northern fault continues westward from Pink Holes Hill for a total inferred distance of about 18.5 km. The fault is not expressed in the Pleistocene surface east of the area 27 access road, where it is only about 250 m north of the medial fault, but is revealed in a few places by deep gully erosion. West of the area 27 access road, the northern fault is marked by scarps in fan remnants and curves to a more southerly strike that projects toward the south side of the Striped Hills (fig. 51).

The medial fault can be traced nearly continuously from Pink Holes Hill westward to the area 27 access road (fig. 51), a distance of about 9 km. The fault, mapped as the "Rock Valley Fault" by Frizzell and Zoback (1987), is approximately parallel to and 2.4 km north of the southern fault. The medial fault continues westward of area 27 for possibly another 7.5 km as a N. 55°–60° E.-trending scarp in Pleistocene alluvium. The fault was trenched by Yount and others (1987). Scarps mapped along the south side of Frenchman Flat (Poole, 1965) imply that the fault also extends approximately 12.5 km eastward from Pink Holes Hill.

The southern fault, which is mapped from near the Mercury Highway westward for a distance of about 14 km (fig. 51), is expressed as several well-exposed scarps, each as much as 2.5 km long. West of Hempell Wash, the fault is exposed in an alluvial fan as two 5- to 7-km-long, parallel splays (northern and southern strands of the southern fault, fig. 51). Farther west, the fault may be represented by lineaments and structures located north and west of the intersection of Jackass Flats Road and the area 27 access road. On the basis of the faults mapped by Barnes and others (1982), the southern fault is inferred to continue about 3 km eastward of the Mercury Highway for a total length of about 17 km.

Trenching Activities

Previous Paleoseismic Work

The Quaternary paleoseismic history of the medial fault in the Rock Valley Fault system was investigated in two trenches (RV1, RV2, figs. 51, 52) that were excavated in 1978 across a 0.5-m-high scarp. Detailed logs of these two trenches were presented by Yount and others (1987) and are not duplicated here; their results indicated at least two episodes of faulting on the fault (as discussed below) that resulted in a total vertical down-to-the-north displacement of 257 to 295 cm. The amount of strike-slip motion that may have been involved could not be determined because of the poorly developed

Figure 52. Surficial geologic map of area surrounding trenches RV1 and RV2 across medial fault of the Rock Valley Fault system in Rock Valley, southwestern Nevada (figs. 1, 2, 51). Map units modified from Hoover and others (1981). Compound units (1ab and so on) denote two lithologic units that cannot be delineated separately at 1:12,000 scale; fractional units (1c/2bc and so on) indicate that a veneer of younger deposits masks, but does not completely conceal, older deposits. Hachured areas, places where land surface has been modified by construction, filling, or excavation. From Yount and others (1987).

DESCRIPTION OF MAP UNITS

[Accompanies fig. 52]

1a **Active wash deposits**—Loose sand and gravel occupying well-defined channel floors. Unvegetated, lacking pavement. Channel form is unmodified. Correlated with unit Q1a of Hoover and others (1981)

1b **Deposits of young washes**—Similar to unit 1a. Generally lies 10 to 50 cm above floors of active washes. Sparsely vegetated. Original channel form is slightly modified. Generally mapped with unit 1a (as unit 1ab) because of scale. Correlated with unit Q1b of Hoover and others (1981)

1c **Young fan and wash deposits**—Sand and gravel composing small alluvial fans and elevated terraces in washes, 1 to 2 m above floors of active washes. Soils have very weak A/Cox profiles. Moderately vegetated. Channel forms are distinctly more subdued than those of unit 1a or 1b. Cobble-bearing debris-flow fronts are locally present on alluvial fans. Correlated with unit Q1c of Hoover and others (1981)

2b **Alluvial-fan and wash deposits**—With surface and lithologic characteristics similar to those of unit Q2 deposits, nested inside and below unit 2c deposits. Generally mapped with unit 2c (as unit 2bc) where slight differences in pavement and drainage development indicate likelihood of deposits of two different ages. Correlated with unit Q2b of Hoover and others (1981)

2c **Intermediate-age alluvial-fan and wash deposits**—Vesicular silt overlying interbedded coarse-grained gravelly sand and sandy gravel. Slight to moderate cementation of sand and gravel by pedogenic carbonate with $CaCO_3$ stage II morphology. Moderate to strong pavement development and moderate dissection, with extensive areas of original depositional surface remaining. Correlated with unit Q2c of Hoover and others (1981)

QTa **Old alluvial-fan deposits**—Indurated, poorly sorted, muddy to sandy cobble and boulder gravel. Moderate to strong cementation by pedogenic carbonate with $CaCO_3$ stages III and IV morphology. Pavement typically is moderately developed, owing to erosional degradation of land surface. Boulders are more common than on unit 2b or 2c surfaces. Carbonate-cemented material is commonly exposed at or near ground surface. Surface is dissected with rounded interfluves. Correlated with unit Qta of Hoover and others (1981)

Tpa **Rocks of Pavit Springs of Hinrichs (1968)**—Interbedded light-gray (10YR 7/2) to pale-brown (10YR 6/3), thin- to thick-bedded siltstone and sandstone and white (10YR 8/2) to light-brown (7.5YR 6/4) silicic tuff and tuff breccia. Siltstone and sandstone contain diatoms and thin ash partings. Fish and plant debris are locally present. Dominantly lacustrine basin-fill deposits, with minor interbeds of fluvial sandstone and conglomerate

bedding and coarse-grained texture of the exposed surficial deposits. No slickensides or other kinematic indicators were observed in the trenches; however, slickensides with a rake of 22° SW. that were observed on a bedrock exposure of the fault plane farther east in Hampel Wash (fig. 51) may indicate a lateral component of fault movement.

The trench in Frenchman Flat (fig. 51), which was excavated on a prominent northwest-facing scarp just east of the Mercury Highway north of Mercury, Nev. (fig. 51), was logged by the second author in 1985. The scarp appears to be on line with the medial or northern fault of the Rock Valley Fault system as projected eastward from central Rock Valley, but an interconnection between the scarp and these two faults is unknown. Stratigraphic and structural relations exposed in this trench are discussed in the next section.

Faults Trenched in 1995

Eight trenches were excavated along the northern and southern faults in the spring of 1995. Four of these trenches were on the northern fault (fig. 51), two perpendicular to the fault (trenches RV3, RV3A) and two parallel to the fault (trenches RV3CT, RV3CT2). Four trenches were excavated on the southern fault, two perpendicular to its northern splay (trenches RV4, RV4A) and two perpendicular to its southern splay (trenches RV5, RV5A). All of these trenches were logged except trenches RV3CT2 and RV5A, which did not intersect the fault.

Surficial geologic maps of the area surrounding the trenches on the northern and southern faults are shown in figures 53 and 54. The surficial deposits (units 1, 2, and so on) were differentiated primarily on the basis of distinct textural, morphologic, and topographic characteristics visible on aerial photographs. Numerical labels were used to indicate a general correlation to the standard stratigraphic sequence (for example, unit 1~unit Qa1, unit 2~unit Qa2, and so on) defined for the Yucca Mountain area (fig. 1; see chap. 2), but do not necessarily imply a precise age equivalency.

At trenches RV3 and RV3A (fig. 51), the northern fault cuts the units 3 and 5–7 geomorphic surfaces, respectively (fig. 53). Trench RV3 is located on a prominent, down-to-the-south scarp (see Swadley and Huckins, 1989). No evidence was observed for lateral displacement of surface features near the trenches. At trenches RV4 and RV5, the southern fault cuts the unit 3/4 geomorphic surface (fig. 54). Although no measurable scarp exists at trenches RV4 or RV5, conspicuous lineaments are visible on aerial photographs.

Trenches were logged by using field and close-range photogrammetric methods (see chap. 1 for details) between April 1995 and January 1996. Stratigraphic units were described by using standard sedimentologic terminology, and soil descriptions follow the nomenclature of Birkeland (1984) and Machette (1985). Offsets of lithologic units across faults, the presence of colluvial wedges or fault fissures, and upward terminations of fractures were interpreted as evidence of paleoearthquakes. U-series and thermoluminescence analyses were used to date lithologic units, soil horizons, and paleoearthquakes, as discussed in chapter 2; estimated numerical ages of samples collected in the trenches are listed in table 39.

Trench Stratigraphy, Structure, and Age Constraints

Logs of six trenches excavated in 1995 are shown on plates 23 through 25, and lithologic-unit and soil-horizon descriptions are listed in tables 40 and 41. The log of the trench at Frenchman Flat is shown on plate 26. Note that the numbering systems for units exposed in trenches are independent from those of the surficial map units shown in figures 53 and 54.

Northern Fault

Trenches on the northern fault expose a sequence of alluvial gravel, colluvium, and eolian sand (pl. 23; table 40). Units in trenches RV3 and RV3CT (fig. 51), which were excavated in middle Pleistocene gravel, are labeled independently from those in trench RV3A, which was excavated in Holocene gravel. In trenches RV3 and RV3CT, five major units are exposed. Units 1 and 3 consist of poorly sorted gravel that is interpreted to be debris-flow deposits. Unit 1 is exposed only in the upthrown block, whereas unit 3 is exposed in both the upthrown and downthrown blocks. Wedge-shaped subunits 3d and 3b, which are present at the fault in the downthrown block, are interpreted to be colluvial deposits. Unit 2, which consists of poorly sorted to well-sorted gravel that is present in both the downthrown and upthrown blocks, is interpreted to be an alluvial-fan flood deposit. Subunit 2a is a channel-fill deposit exposed in trench RV3CT. The thalweg of the buried channel at the base of unit 2a is used to estimate the cumulative fault slip, as described below. Unit 4, consisting of moderately well sorted to well-sorted sand that is present only in the downthrown block, thins away from the fault. A few reworked fragments of unit 4 are visible on the upthrown block, indicating that the unit may have been stripped from the upthrown block. Unit 4 is interpreted to be an eolian deposit that has undergone some alluvial and (or) colluvial reworking. Unit 5 consists of silty eolian sand that is present on both sides of the fault.

Exposed soils include an Avk horizon on unit 5, a Bkw to Btw horizon on unit 4, and two silica-carbonate soils, one formed on units 2 and 3 and one on unit 1 (table 41). The top of the youngest carbonate soil forms a conspicuous, stripped, irregular boundary with overlying unit 5 on the upthrown block but is continuous and diffuse with overlying units 4 and 5 on the downthrown block.

Age constraints on units 1 through 5 include one thermoluminescence age on a sample (TL–57, 12±5 ka, pl. 23; table 39) from unit 5 and three U-series ages on samples

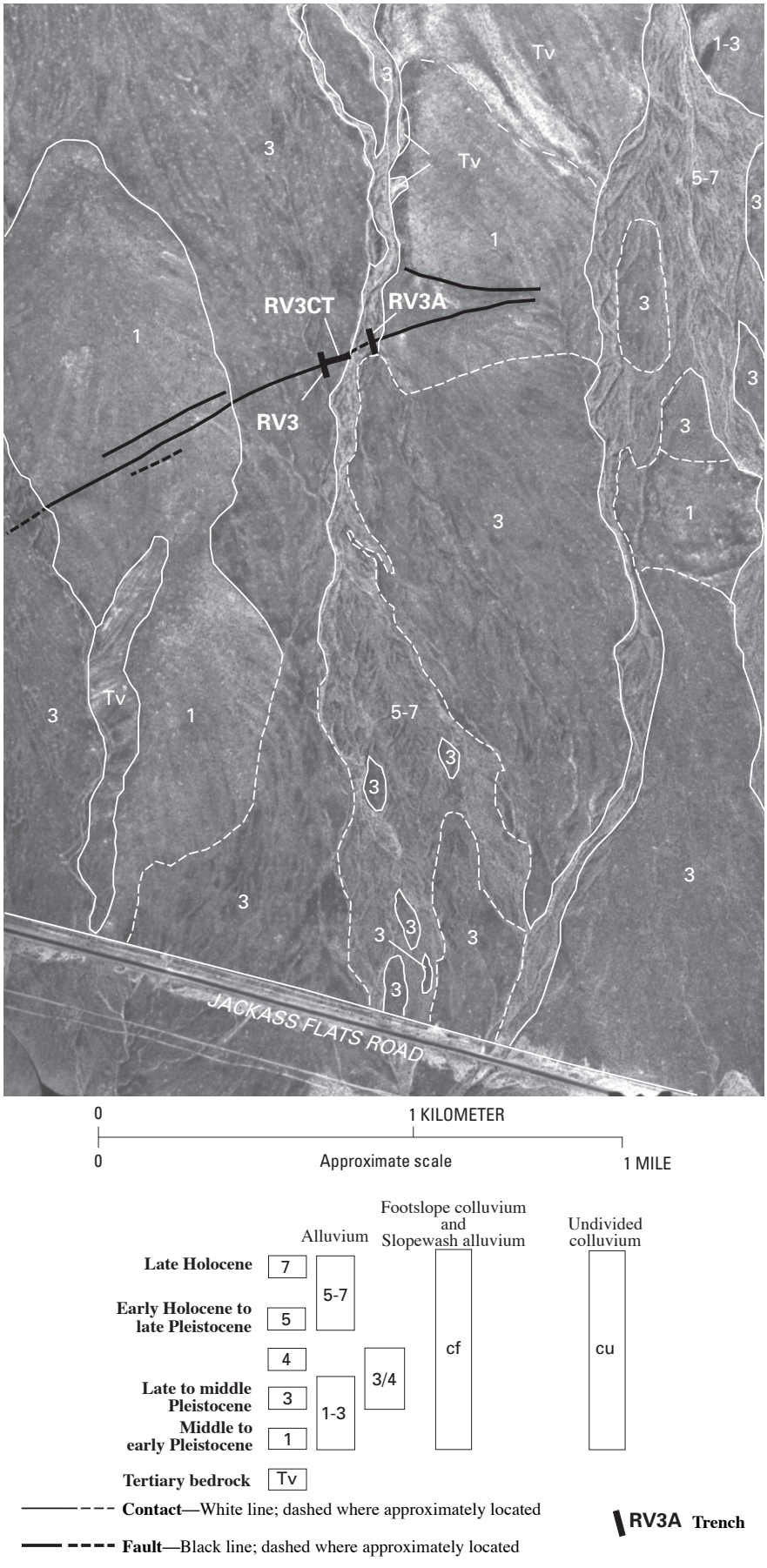

Figure 53. Surficial geologic map of area surrounding trenches RV3, RV3CT, and RV3A across northern fault of the Rock Valley Fault system in Rock Valley, southwestern Nevada (pl. 23; figs. 1, 2, 51).

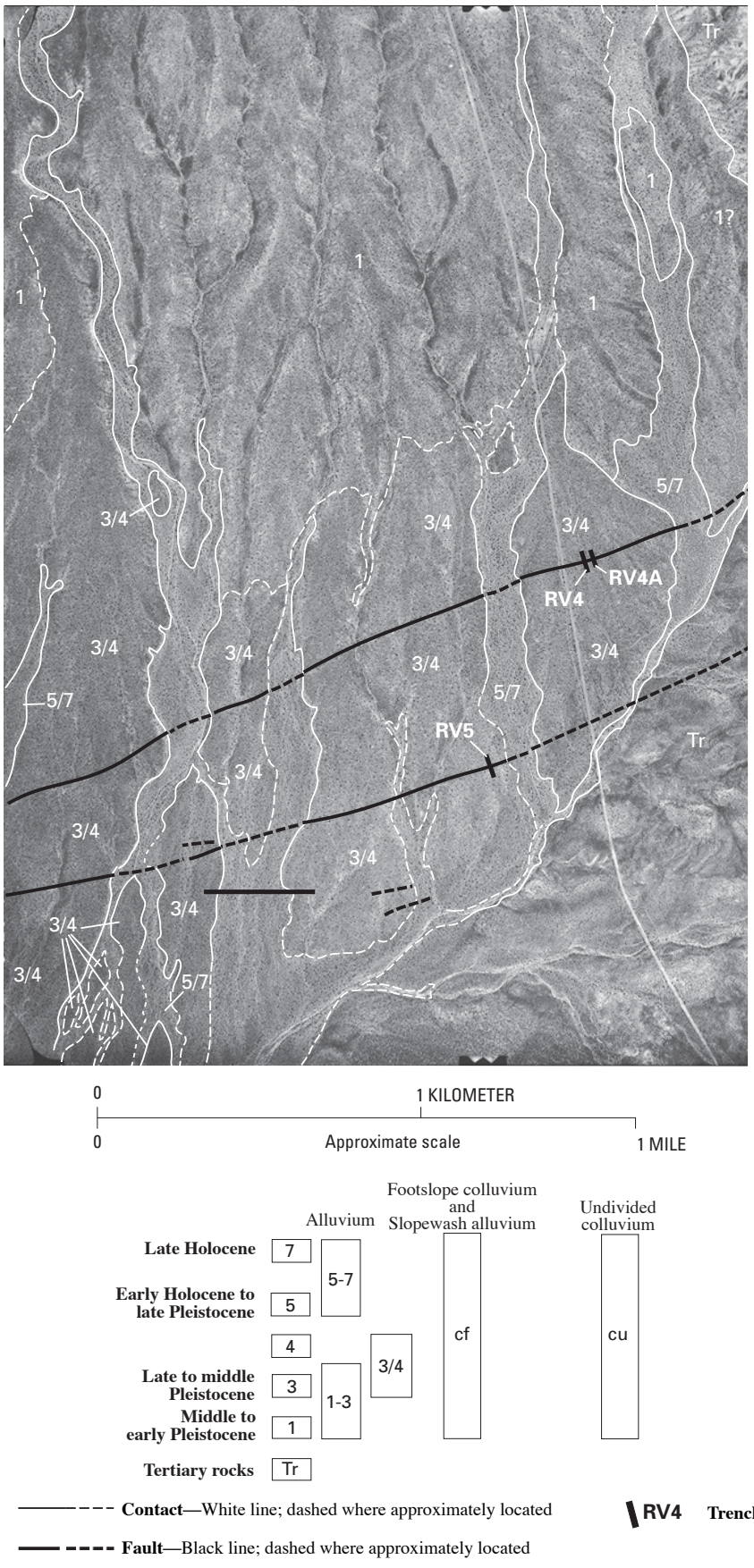

Figure 54. Surficial geologic map of area surrounding trenches RV4, RV4A, and RV5 across northern and southern splays of southern fault of the Rock Valley Fault system in Rock Valley, southwestern Nevada (pl. 24; figs. 1, 2, 51).

Table 39. Numerical ages of deposits exposed in trenches RV2, RV3, RV3A, RV4, and RV5 and in the trench in Frenchman Flat (FFT1) across the Rock Valley Fault system in the Yucca Mountain area, southwestern Nevada.

[See figures 1, 2, and 51 for locations. Samples: TL– (error limits, ±2σ), thermoluminescence analyses by S.A. Mahan; HD (error limits, ±2σ), U-series analyses by J.B. Paces. Do., ditto]

Trench	Sample	Unit and material sampled	Estimated age (ka)
RV 2[1]	TL–74	Base of 3Btkb2 soil horizon	47±4
	TL–75	Av soil horizon	7±1
RV 3	TL–57	5, buried Av soil horizon	12±5
(pl. 23)	HD 1812	3f, upper platy K soil horizon	74±13, 79±3
	HD 1955	3a, silica-rich clast rind	98±2, 102±3, 106±2
RV 3CT	HD 1954	1, silica-rich clast rind	367±55, 550±270
(pl. 23)			
RV 3A	TL–58	8, sandy lens	11±2
(pl. 23)			
RV 4	TL–53	5, buried Av soil horizon	2±0.5
(pl. 24)	TL–54	2e, sandy lens in alluvium	88±74, 92±62
	HD 1803	2e, rhizolith	26.5±0.2
	HD 1804	3, clast-rind K soil horizon	35±1, 50±1, 64±2
	HD 1805	3, opaline silica stringer in K soil horizon	16.4±0.3
RV 5	TL–55	Fissure fill	10±1
(pl. 25)	TL–56	Do	6±1
	HD 1807	Opaline silica laminae in fissure fill	10±2, 12±4, 46±9, 72±10
	HD 1809	1c, laminar K soil horizon	321±44
	HD 1810	Fissure fill, top of K soil horizon	9±3, 10±5
	HD 1811	1e, laminar K soil horizon	22.4±0.8, 50.0±2.6
FFT 1	TL–72	B, eolian fill	9±1
(pl. 26)	TL–73	B, Bk soil horizon	27±2

[1]Trench log not included in this report.

from the two silica-carbonate soils formed on units 1 through 3. One sample (HD 1812), from silica-carbonate rinds on clasts at the top of unit 3 on the downthrown block, yielded ages of 74±13 and 79±3 ka, indicating that the unit 3 deposits are older than 79 ka. A second sample (HD 1955), from near the base of unit 3 on the downthrown block, yielded an average age of 102±2 ka, indicating that the oldest part of unit 3 is older than 100 ka. A third sample (HD 1954), from unit 1 on the upthrown block near the base of trench RV3CT (fig. 51), yielded ages of 550±270 and 367±55 ka. These ages, in combination with ages from unit 3 and an estimated time interval represented by the erosion that occurred on the top of unit 1, indicate that unit 2 was probably deposited sometime between about 300 and 100 ka.

The fault exposed in trenches RV3 and RV3CT (fig. 51) is expressed primarily as a fissure filled with cobbly colluvium (fig. 55). The fissure narrows with depth and ranges in width from about 70 cm near the top of the B soil horizon to about 10 cm at the base of the trench. Units 1 through 4 are offset down to the south across the fissure. The fault strikes N. 66° E. and dips vertically at the trench site. Striae with a rake of 11° NE. (pl. 23) indicate that the downthrown (southern) block moved northeastward during at least one episode of Quaternary fault movement. The cumulative horizontal and vertical displacements that have occurred along the fault since middle to late Pleistocene time, which were estimated by using the thalweg of the channel at the base of unit 2a in trench RV3CT (pl. 23), are 14.2 and 1.2 m, respectively.

Trench RV3A (fig. 51) was excavated in lower to upper Holocene alluvium in an attempt to determine the timing of the most recent paleoearthquakes on the northern fault. The trench exposes a fault zone composed of two shear zones, the youngest of which is capped by a sequence of colluvial-wedge deposits (units 7a–7d, pl. 22; fig. 56). A thermoluminescence analysis of a sample (TL–58, table 39) from the lower part of overlying unit 8 yielded a date of 11±2 ka, which is interpreted to indicate that the unit was deposited approximately contemporaneously with unit 5 (12 ±5 ka) in trenches RV3 and RV3CT (fig. 51).

Table 40. Summary of the characteristics of lithologic units exposed in trenches across the Rock Valley Fault system in the Yucca Mountain area, southwestern Nevada.

[See figures 1, 2, and 51 for locations and table 41 for soil descriptions. Position: FW, footwall; HW, hanging wall. General lithology and matrix: bld, boulder; c, coarse; cbl, cobble; f, fine; gvl, gravel; m; medium; pbl, pebble; slt, silt; snd, sand. Deformation: EW, event wedge; F, faulted. Do., ditto]

Unit	Position	General lithology	Clast size (cm)	Matrix	Cementation	Thickness	Shape	Deformation	Interpretation
					Trench RV3, west wall				
5	HW	slt snd	<50	f snd	See soil description ---------	See soil description -----	Tabular ----------	F	Eolian material.
4	HW	bld cbl pbl snd	<40	snd	do ----------	do ----------	Wedge ----------	F	Do.
3	HW	bld cbl snd pbl grv	15 (max 100)	snd	do ----------	do ----------	Lenticular ----------	F	Debris-flow deposits.
2	HW	bld cbl snd pbl grv	10 (max 50)	c snd	do ----------	do ----------	Tabular ----------	F	Alluvial gravel.
					Trench RV3A, east wall				
1	FW	snd bld cbl grv	0.2–40	m-c snd pbl	$CaCO_3$, stage III–IV -----	>50 (from floor)	Tabular ----------	F	Alluvial gravel.
2	FW	cbl pbl snd gvl	.2–10	pbl	$CaCO_3$ stage II ----------	60	do----------	F	Do.
3	FW	cbl bld snd	.2–40	m-c snd	$CaCO_3$ stage II–III -------	20–50	do----------	F	Debris-flow deposits.
3	HW	pbl cbl snd	.2–15	m-c snd	$CaCO_3$ stage II–III -------	>35	do----------	F	Do.
4	FW	pbl cbl bld snd gvl	1	pbl	$CaCO_3$ stage II–III -------	0–45	Lenticular ----------	F	Alluvial gravel.
5	HW	pbl snd cbl gvl	.2–10	pbl	$CaCO_3$ stage I ----------	0–50	Wedge ----------	EW	Alluvial/colluvial wedge.
6	HW	pbl cbl snd to snd pbl cbl gvl	.2–30	m-c snd pbl	$CaCO_3$ stage I ----------	20–70	Irregular ----------	F	Alluvial gravel.
7	HW	snd cbl pbl gvl	.2–40	m-c snd pbl	$CaCO_3$ stage <I----------	0–40	Wedge ----------	EW	Colluvial/eolian wedge.
8	HW	pbl cbl snd	.2–5	m-c snd	$CaCO_3$ stage <I----------	0–70	Lenticular ----------	None	Alluvial sand and gravel.
9	HW	pbl snd cbl gvl	.2–30	pbl	$CaCO_3$ stage <I----------	0–50	Tabular ----------	None	Do.
10	FW & HW	snd cbl bld pbl grv	.2–55	m-c snd	$CaCO_3$ stage I ----------	0–70	do----------	None	Do.
11	FW & HW	pbl cbl snd	.2–40	m-c snd	$CaCO_3$ stage I ----------	40	do----------	None	Do.
					Trench RV4, west wall				
1	FW–HW	snd cbl pbl gvl	<14	snd	See soil description ------	>30	Tabular ----------	F	Alluvial sand and gravel.
2	FW–HW	cbl pbl snd	1–10	snd	do ----------	See soil description ----	do----------	F	Do.
3	FW–HW	snd cbl pbl gvl	2–6	snd	do ----------	do ----------	do----------	F	Do.
4	FW–HW	cbl pbl snd	7–10	snd	do ----------	do ----------	do----------	F	Eolian material.
5	FW–HW	slt snd	7–10	snd	do ----------	do ----------	do----------	F	Do.
					Trench RV5, west wall				
1a	FW–HW	gvl snd	0.2–2	f-c snd	See soil description ------	>20	Tabular ----------	F	Alluvial gravel.
1b	FW–HW	gvl snd	<1	f-c snd	do ----------	0–10	do----------	F	Do.
1c	FW–HW	snd gvl	<2	f-c snd	do ----------	30–50	do----------	F	Alluvial sand and gravel.
1d	FW–HW	snd cbl gvl	.2–15	f-c snd	do ----------	0–35	Lenticular-tabular.	F	Alluvial deposits.
1e	FW–HW	gvl snd	.2–5	f-c snd	do ----------	40–60	Tabular ----------	F	Do.
2	FW–HW	pbl snd	.2–10	f-m snd	do ----------	See soil description -----	do----------	F	Eolian material.
3	FW–HW	slt snd	.2–3	f-m snd	do ----------	do ----------	do----------	Fractured only	Do.

Northern Strand of the Southern Fault

Trenches RV4 and RV4A (fig. 51), which were excavated across the northern splay of the southern fault, expose a sequence of middle to upper Pleistocene alluvial sand and gravel and younger eolian sand (pl. 24; table 40). The two trenches expose the same five major units on both sides of the fault, labeled by using the same numbering scheme. Units 1 through 3 are interpreted to be alluvial-fan flood deposits, and units 4 and 5 are interpreted to be silty sand of eolian origin. Soils exposed in the trench include Avk and B horizons on unit 5, a buried Bw horizon on unit 4, and two buried silica-carbonate soils, one formed on units 3 and 2 and one on unit 1 (table 41).

Estimated ages for units 1 through 5 are based on one thermoluminescence analysis of a sample from unit 5, two U-series analyses of samples from the silica-carbonate soil formed on unit 3, and one thermoluminescence and one U-series analysis of samples from unit 2 (table 39). The thermoluminescence analysis, of a sample (TL–53, pl. 24; table 59) from unit 5, yielded an age of 2±0.5 ka; and the U-series analysis, of a sample (HD 1804) from the inner rind on a clast, yielded a maximum age of 64±2 ka. Another sample (HD 1805), from a silica-rich soil stringer, gave an age of 16.4±0.3 ka. Because sample HD 1804 was from the inner rind of a clast, we assume that its age is closer to the date of earliest soil formation on unit 3 than is that of sample HD 1805; therefore, we consider unit 3 to have been deposited before 62 ka. The two samples (TL–54, HD 1803) from unit 2 were from the silty-sand matrix and a silica-carbonate rhizolith, respectively. Sample TL–54 yielded ages of 88±74 and 92±62 ka, and sample HD 1803 an age of 90±74 ka. Despite the large error limits, we interpret these ages to indicate that unit 2 was deposited probably about 90 ka; the ages also imply that unit 3 was deposited about 90–62 ka.

The fault exposed in trenches RV4 and RV4A (fig. 51) is expressed as a zone of three to five fault strands that together range in width from about 1.7 m near the base of the trench to about 4.6 m near the top (pl. 24). Vertical-slip displacement along the fault appears to be slightly down to the north. All units are exposed on both sides of the fault zone (fig. 57). Although all units are cut by the fault strands, the cumulative vertical separation is less than 30 cm. The overall strike of the fault at the trench sites is N. 71° E., and various strands dip from about 45° to near vertical. The fault zone in both trenches has been disrupted by bioturbation, primarily from burrowing animals. In trench RV4A, the zone of disruption surrounding the fault is about 10 m wide. No striae were observed in either trench.

Southern Strand of the Southern Fault

Trench RV5 (fig. 51), which was excavated on the southern splay of the southern fault, exposes a sequence of alluvial sand and gravel, as well as eolian sand (pl. 25; table 40). Three major units are exposed: unit 1, which grades from sandy gravel to gravelly sand, is interpreted to be an alluvial-fan flood deposit; and units 2 and 3 consist of silty eolian sand. Exposed soils include an Av horizon on unit 3, a buried Bt horizon on unit 2, and a silica-carbonate soil ($CaCO_3$ stage II–IV morphology) on unit 1 (table 41).

Estimated ages for unit 1 are provided by two U-series analyses (pl. 25; table 39): (1) sample HD 1809, from a silica-rich rind on a clast in unit 1c, yielded ages of 324±275 ka and 321±44 ka; and (2) sample HD 1811, from a silica-rich platy horizon in unit 1e, yielded ages of 22.4±0.8 and 50.0±2.6 ka. Earlier studies of calcic-soil formation (for example, Machette, 1985) reported that such well-developed carbonate soils as that observed in trench RV5 (fig. 51) can take hundreds of thousands of years to develop. We interpret the 20–50-ka ages, therefore, to reflect a relatively late influx of silica and carbonate into the deposits, rather than an early influx closer in time to the age of the sediment. We consider the 320-ka age to be most representative of the oldest carbonate in the deposits, and so we date unit 1 at older than 320 ka.

In trench RV5 (fig. 51), the southern splay of the southern fault is expressed as a zone of four fault strands, most of which have shear fractures that are carbonate cemented and terminate at or near the top of unit 1e (figs. 53, 54). One shear zone appears to terminate at the base of unit 1e on the west wall but at the top of unit 1e on the east wall. Striae along one of the shears have a rake of 17° SW. Two of the fault strands have fissures filled with silty sand that are younger than the carbonate-cemented shear zones. The largest fissure, which ranges in width from about 5 cm near the base of the east wall to about 35 cm near the top (fig. 58), truncated and split a previously existing carbonate-cemented shear zone. Units 1 and 2 are cut and vertically offset, down to the north, by the fault strand with the widest fissure and carbonate-cemented shear zone. Cumulative vertical displacement measured at the top of unit 1 ranges from 12 to 22 cm. Unit 3 is cut by a fracture that extends upward from one of the fault strands exposed on the west wall (fig. 58). No shear offset is visible along this fracture, and so it may be pedogenic rather than tectonic.

A thermoluminescence analysis of a sample (TL–55, table 39; 10±1 ka) from unit 3, which is the fill in the widest fissure about 0.7 m below the ground surface, indicates that the fissure began filling about 10 ka and that unit 2 is older than 10 ka because blocks of unit 2 are mixed in with the unit 3 deposits (pl. 25). Another sample (TL–56), from a younger part of the fissure fill about 0.3 m below the ground surface, yielded an age of 6±1 ka. U-series ages on two samples (HD 1807, 72±10, 46±9, 12±4, 10±2 ka; HD 1810, 10±5, 9±3 ka) from silica-rich laminae along the edges of unit 1e that line the fissure indicate that the youngest silica-carbonate coating on the fissure is dated at about 9–11 ka, or about contemporaneous with the oldest fissure fill (unit 3). The older U-series ages on these samples may have resulted from obtaining the samples from coatings that existed in the carbonate-cemented shear zone before splitting by the fissure.

Table 41. Descriptions of soil profiles in trenches across the Rock Valley Fault system in the Yucca Mountain area, southwestern Nevada.

[See figures 1, 2, and 51 for locations. See table 3 for soil-horizon terminology. Colors from Munsell Soil Color Charts (Munsell Color Co., Inc., 1992). Texture: lm, loam; snd, sand. Structure—grade: 1, weak; 2, moderate; 3, strong; m, massive; sg, single grain—size: c, coarse; f, fine; m, medium; v, very fine—type: abk, angular blocky; pl, platy; sbk, subangular blocky. Consistence—dry: eh, extremely hard; h, hard; lo, loose; sh, slightly hard; so, soft; vh, very hard—wet: po, nonplastic; ps, slightly plastic; so, nonsticky; ss, slightly sticky. CO_3 stage morphology from Birkeland (1984). Effervescence (in cold dilute HCl): e, some; em, moderate; eo, none; es, strong; ev, very strong; vse, very slight. Cementation: ci, indurated; cs, strong; cw, weak. Lower horizon boundary—distinctness: a, abrupt; c, clear; g, gradual—topography: i, irregular; s, smooth; w, wavy. Roots—abundance: 1, few, 2, common—size: co, coarse; f, fine; m, medium; vf, very fine. Rhizoliths—abundance: 1, few. NA, not available; n.o., not observed]

Horizon	Depth (cm)	Associated unit	Color		Gravel content (wt pct)	Text	Structure	Consistence		CO_3 stage morphology	Effervescence	Cementation	Lower horizon boundary	Roots	Rhizoliths
			Wet	Dry				Dry	Wet						
Soil profile RV3–SPI															
Avk	0	5	10YR 4/4	10YR 6/3	3–5	sndlm	2 vco pl-sbk	sh	ss ps	n.a.	ev	n.o.	c s	1 vf-m thruout	n.o.
Bkw	16	5	10YR 3/4	10YR 6/3	5–10	sndlm	3 m-co sbk	sh-h	vss vps	I	ev	cs	a s	1-2 vf-m thruout	n.o.
2Btwk	48	4	7.5YR 3/4	7.5YR7/3	3–5	lmysnd	3 m-co pl	vh	so po	I	ev	cw	a w	1 f-m	n.o.
2Kqm	72	3	7.5YR 6/3	7.5YR8/1	10	lmysnd	3 vco-pl	eh	so po	IV	eh	ci	c i	1 vf	n.o.
2K	89	3	10YR 4/2	10YR7.5/1	50	lmysnd-snd	m-sg	lo	so po	II+–III	ev	cs	c s	1 vf	1
3Bk	175	2	10YR 3/1	10YR6/1	60	lmysnd-snd	sg	lo	so po	II	ev	n.o.	Bottom	n.o.	n.o.
Soil profile RV3–SPII															
Ak	0	5	10YR 4/3	10YR7/3	10	sndlm	1f-m sbk	so	ss-ps	I	ev	n.o.	a w	1vf-m	n.o.
2K	20	3	10YR 5/6	10YR7/2	50	snd	m	h	so po	III	ev	cs	a w	1 vf-f thruout	n.o.
B+K	121	2	10YR 4/2	10YR7.5/1	60–70	snd	sg	lo	so po	I–III	ev	n.o.	a s	1 vf-f	n.o.
3Kq	273	1	10YR 5/3.5	10YR7/2	70	lmsnd	m-sg	h	so po	III	ev	cs	Bottom	1 vf	n.o.
Soil profile RV4–SPI															
Avk	Top	– –	10YR 5/4	10YR 5/2	5	sndlm	2 vco-pl	sh	vssvps	– –	ev	n.o.	a w	1 vf thru-out	n.o.
B	8	5	10YR 4/4	10YR 6/3	5–10	sndlm	2 m-co sbk	sh	vss vps	– –	eo	n.o.	a s	1 vf-co thruout	n.o.
2Bwbl	18	5	10YR 3	10YR 6/4	40–50	sndlm	3 co-abk	h	so po	– –	vse	n.o.	a s	1 m-co thruout	n.o.
2Kqmbl	34	4	10YR–7.5YR 6/4	10YR 8/0– 8/3	40–50	sndlm	3 vco-pl	eh	so po	IV	ev	cs-ci	a w	1 vf	n.o.
2Kbl	48	3	10YR 5/2	10YR 8/2	50	lmsnd	1–2 f-m sbk	lo so	so po	III	ev	cs	c w	1 m	1
2Bkbl	96	3	10YR	10YR	60	lmsnd	m-sg gr	lo	so po	I–II+	ev	cs	a s	1 f-m	1
3Bkbl	141	2	10YR 4/3	10YR 7/2	40–50	lmsnd	sg gr	lo	so po	I	ev	cs	a s	1 f snd lenses	1
4Bkb2	265	1	10YR 4/3	10YR 7/3	40–50	lmsnd	1 vf sbk	lo	so po	II–III–	ev	cs	Bottom	1 f	n.o.
Soil profile RV5–SPI															
Av	0	3	10YR 5/3	10YR 7/3	5	sndlm	3 vco pl	sh	vss vps	– –	sh	NA	a s	1 vf	n.o.
2Btbl	19	2	7.5YR 4/4	10YR 6/4	10	sndlm	2 m abk	sh-h	so po	– –	ev	NA	a w	1 f-m thruout	n.o.
3Kqmbl	37	1	10YR 7/2	10YR 8/2	30–40	lmsnd	3 vco pl	eh	so po	IV	ev	ci	c w	1 f	n.o.
3Kbl	64	1	10YR 7/2	10YR 8/2	20	lmsnd	m	eh	so po	III	ev	ci	c w	1 f	n.o.
3bk	102	1	10YR 4/3	10YR 7/2	40	lmsnd	m-sg	lo	so po	I–II	ev	cs	NA	None	1

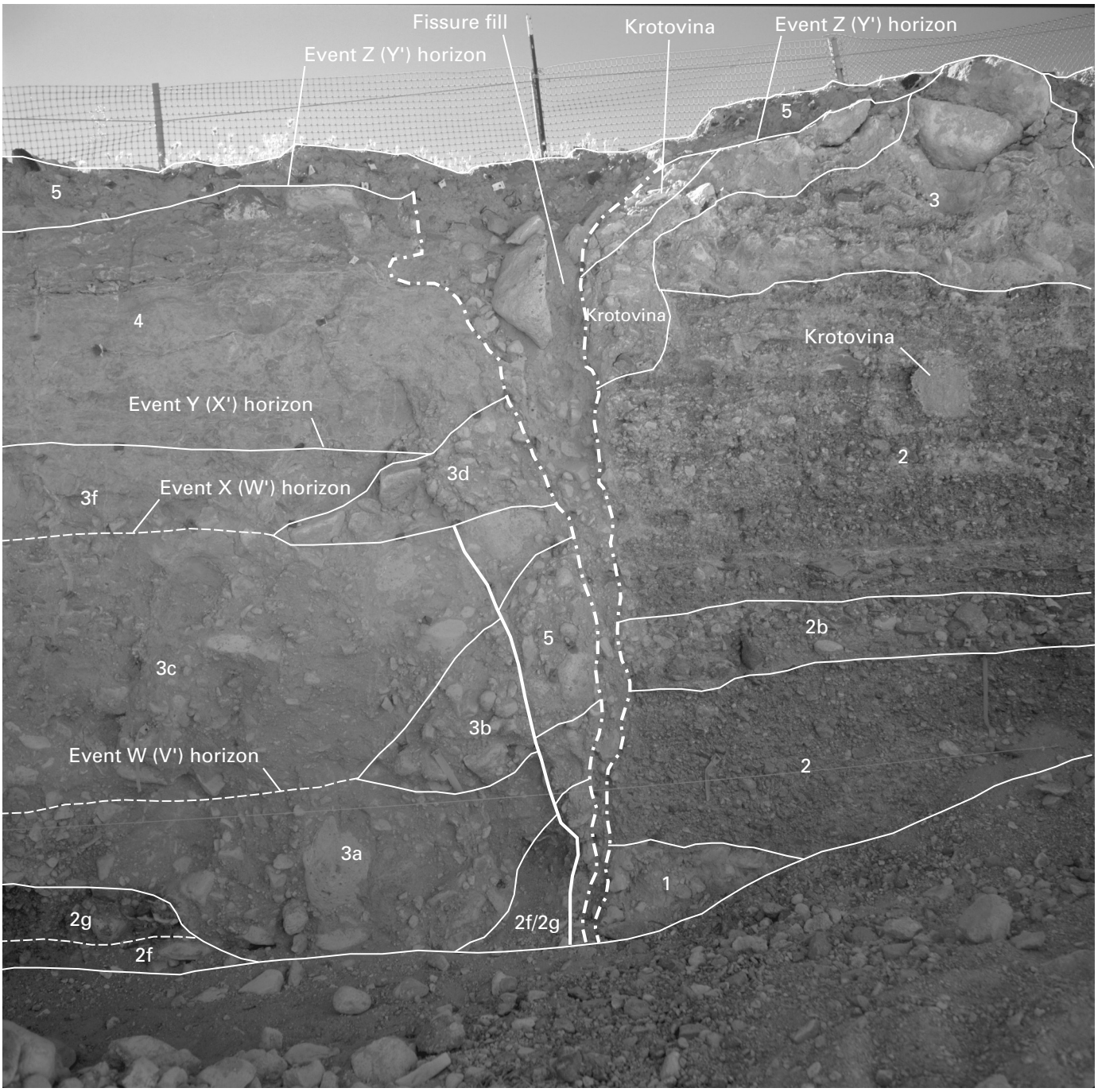

EXPLANATION

Fissure boundary

Fracture

Lithologic-unit boundary—Dashed where approximately located

2f **Lithologic unit**

Figure 55. Part of west wall of trench RV3 across northern fault of the Rock Valley Fault system in Rock Valley, southwestern Nevada (pl. 23; figs. 1, 2, 51). Faulting-event horizons are labeled according to both local- and fault-system-wide-event (in parentheses) schemes. No evidence for event Z′ was observed on northern fault strand. Trench wall is about 3 m high.

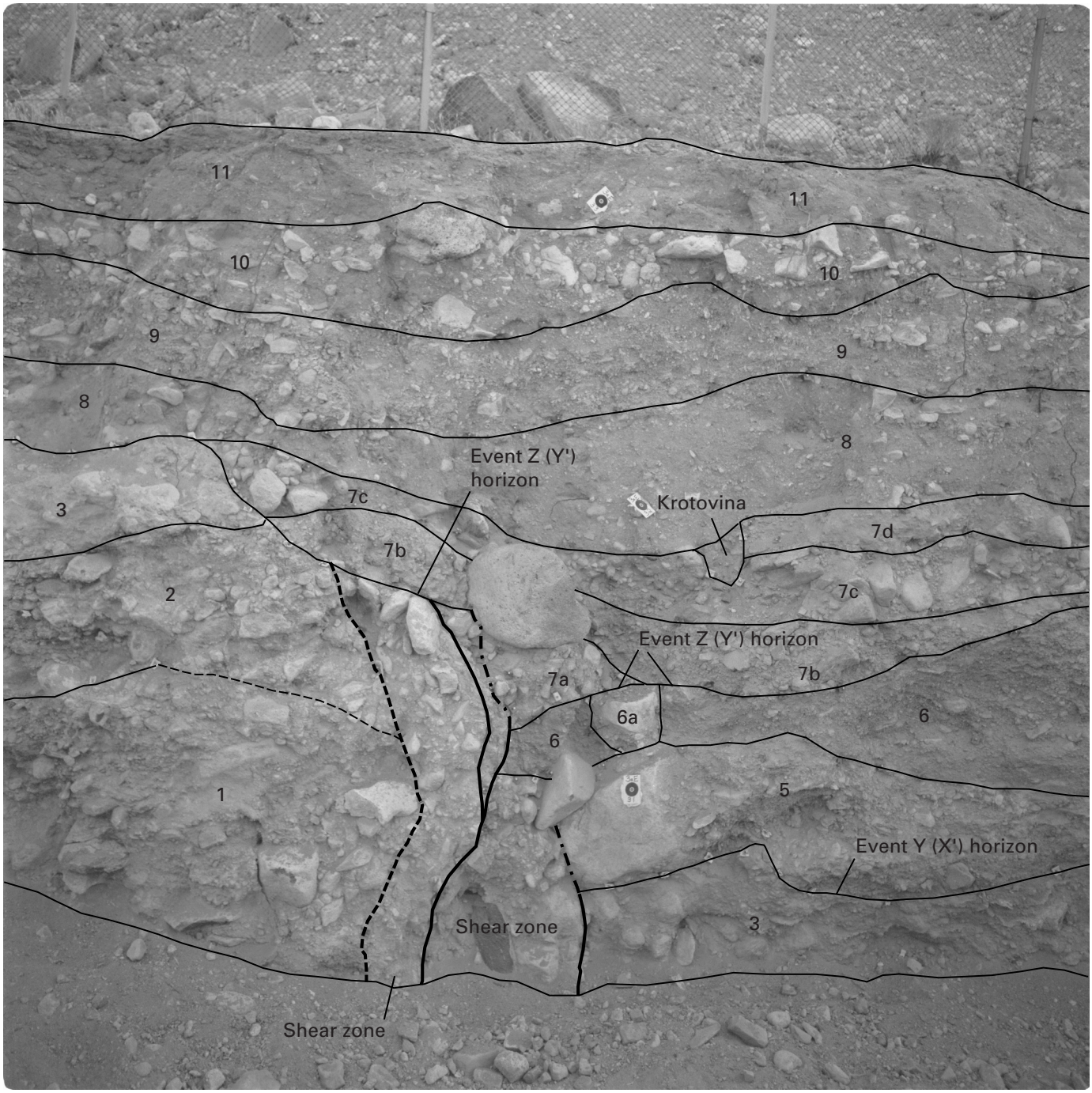

EXPLANATION

Free face

Fracture—Dashed where appoximately located

Lithologic-unit boundary—Dashed where approximately located

3 **Lithologic unit**

Figure 56. Part of east wall of trench RV3A across northern fault of the Rock Valley Fault system in Rock Valley, southwestern Nevada (pl. 23; figs. 1, 2, 51). Faulting-event horizons are labeled as in figure 58.

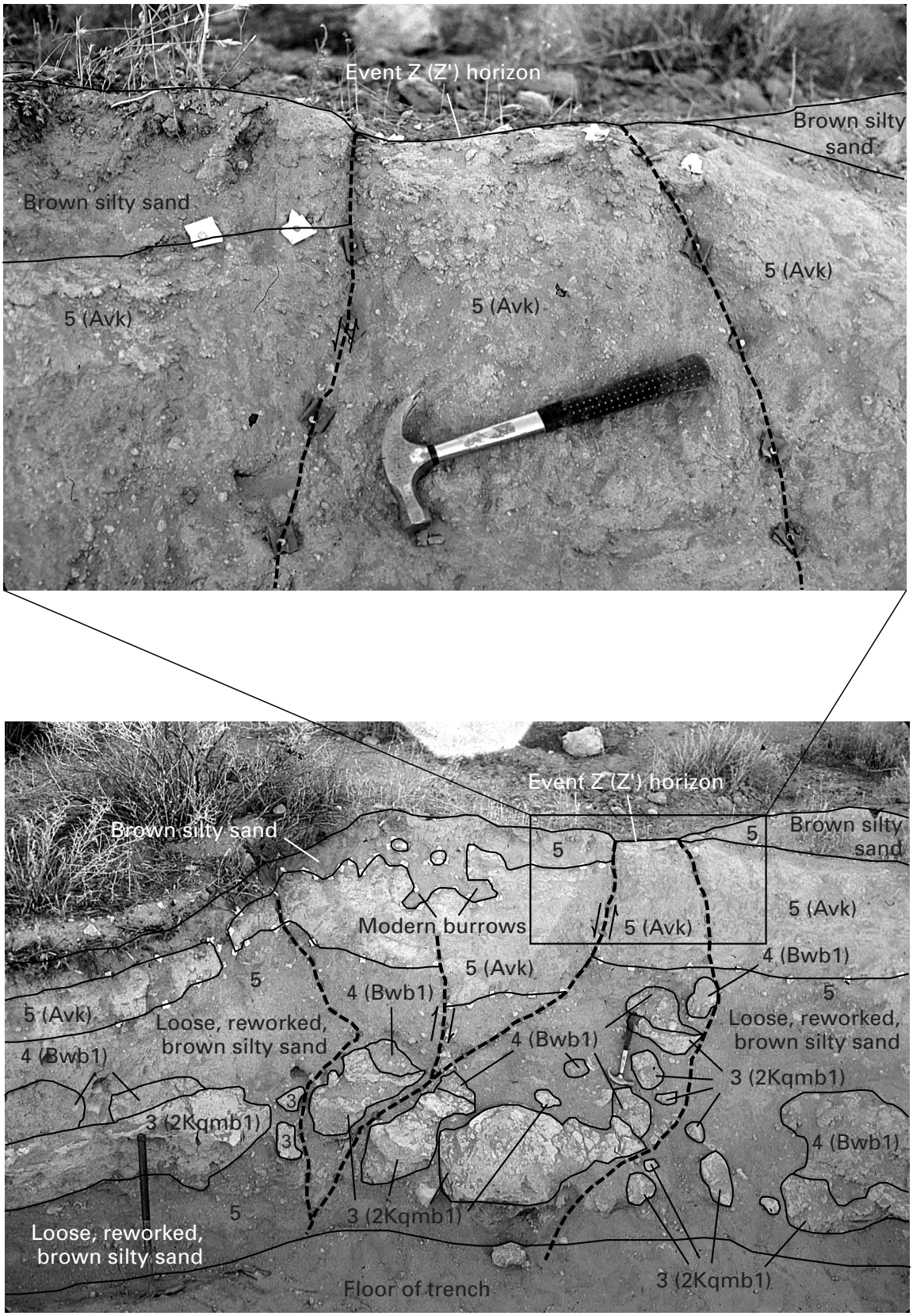

Figure 57. Central part of west wall of trench RV4A across northern strand of southern fault of the Rock Valley Fault system in Rock Valley, southwestern Nevada (pl. 24; figs. 1, 2, 51). Upper photograph shows detailed area outlined in lower photograph. Faulting-event horizons are labeled as in figure 58.

Frenchman Flat Fault

The trench in Frenchman Flat (fig. 51) exposes a sequence of sandy alluvial-fan gravel and eolian sand (pl. 26). Three major units were distinguished on the west wall of the trench: unit C, which consists of sandy gravel exposed on the lower part of the wall, is interpreted to be an alluvial-fan flood deposit; and units B and A, composed of silty sand, are interpreted to be primarily of eolian origin. Soils exposed in the trench include an Av horizon on unit A, a Bw horizon on unit B, and a moderately well cemented silica-carbonate horizon on unit C.

The Frenchman Flat Fault is expressed as a graben that downdrops units C and the Bw soil horizon of unit B; the overall sense of displacement is down to the north. The Bw soil horizon is visible in the graben but is covered by about 1 m of slopewash and eolian deposits mapped as a younger part of unit B with a less pronounced soil color. A thermoluminescence analysis of a sample (TL–73, table 39) from the Bw soil horizon exposed in the graben yielded an age for the part of unit B offset by the fault of about 27±2 ka. A thermoluminescence analysis of a sample (TL–72, table 39) from the sediment fill directly above the Bw soil horizon exposed in the graben yielded an age of 9±1 ka, indicating that the graben began filling at 10–8 ka.

Paleoseismic Interpretations

Chronology of Surface-Rupturing Paleoearthquakes

Evidence for paleoearthquakes, age constraints, and displacement data for each fault (or fault splay) are summarized in table 42. Paleoearthquakes are labeled in two ways: (1) a local-event-labeling scheme (events Z, Y, X, and so on, from youngest to oldest) that is unique to each fault or fault splay, and (2) an interpretative, fault-system-wide-event-labeling scheme using a prime (′). For example, five faulting events (Z–V) were identified in trenches on the northern fault, with event Z dated at about 13±4 ka. On a fault-system-wide basis, however, evidence was observed for one faulting event on the southern fault dated at about 2±0.5 ka, or about 10 k.y. later. Thus, event Z on the northern fault would have an interpretative label of Y′, identifying it as the penultimate faulting event in the paleoseismic record for the total Rock Valley Fault system. According to this interpretative scheme, event Y on the northern fault is labeled X′, event X is labeled W′, event W is labeled V′, and event V is labeled U′. In the following paragraphs, we discuss the temporal correlation of paleoearthquakes on a fault-system-wide basis. Evidence, age control, and our attempt at fault-system-wide-event correlation are considered to be most reliable for the most recent (Z′) and penultimate (Y′) faulting events. Where evidence for local events was documented at the same soil horizon (for example, B) on multiple faults, these events were grouped together as a single fault-system-wide event if age control was adequate for this purpose. Because this technique is generalizing, the fault-system-wide events described below are considered to be the minimum number within the entire Rock Valley Fault system.

Event Z′

Evidence for event Z′ was observed on the northern splay of the southern fault where the A soil horizon was vertically offset (table 42). Possible evidence for the event was observed on the medial fault and the southern splay of the southern fault where the A soil horizons were fractured but not vertically offset. A thermoluminescence analysis of a sample (TL–53, table 39) from the A soil horizon in trench RV4 (fig. 51) on the northern splay of the southern fault is interpreted to date event Z′ at later than 2±0.5 ka. In trenches on the medial fault and on the southern splay of the southern fault, the event is constrained to be younger than 7±1 ka (sample TL–75, trench RV2) and 6±1 ka (sample TL–56, trench RV5), respectively. Although the age constraints for each fault do not precisely correspond, we interpret the evidence to indicate that only one faulting event is represented because its stratigraphic position is the same in all the trenches—that is, at the top of the A soil horizon (see figs. 55, 57, 58). Total net displacement from event Z′ was probably less than 10 cm on both splays of the southern fault. If the event occurred on the medial fault, displacement was probably similar to that on the southern fault.

Event Y′

Evidence for event Y′ was observed in all the trenches (table 42). The event horizon was within or at the top of the B (Bk to Bt) soil horizon (pls. 24, 26; figs. 55, 58), except in trench RV3A, which was excavated in Holocene channel deposits (fig. 56). In general, thermoluminescence and U-series ages indicate that event Y′ probably occurred sometime between 72 and 7 ka. The timing is best constrained on the northern fault in trenches RV3 and RV3A (pl. 23), where the ages indicate that the event occurred about 13±4 ka. The length of the surface rupture associated with event Y′ was at least 23 km—the distance from the trench in Frenchman Flat trench to trench RV3 at the southwest end of the northern fault in central Rock Valley. Displacement along the northern fault was left lateral, down to the south; displacement along the southern and medial faults was left lateral, down to the north; and displacement along the Frenchman Flat Fault was down to the south, with an unknown strike-slip component. Total net displacements ranged from less than 10 cm on the northern splay of the southern fault to 267 cm on the northern fault.

Event X′

Evidence for event X′ was also observed in trenches on all faults (table 42). The event horizon is at or near the top

of the silica-carbonate soil horizon (pls. 24, 25; fig. 55). Its date is most tightly constrained in trench RV4 to 64–16 ka (samples HD 1804, HD 1805, table 39) on the northern splay of the southern fault, with a median value of 40±24 ka. Vertical displacement on the northern fault was down to the south, whereas along the medial and southern faults it was down to the north. Displacements for event X′ ranged from less than 10 cm on the northern splay of the southern fault to less than 362 cm on the northern fault.

Events W′ and V′

Evidence for events V′ and W′ was observed only in trench RV3 (fig. 57) on the northern fault (fig. 55; table 42). Both events are documented by colluvial wedges within unit 3. In a gross sense, U-series ages constrain the dates of both events at about 300–80 ka. However, because the best estimated age for the lower part of unit 2 (unit 2a) is 200 ±100 ka, we date the deposition of unit 3 at about 200–80

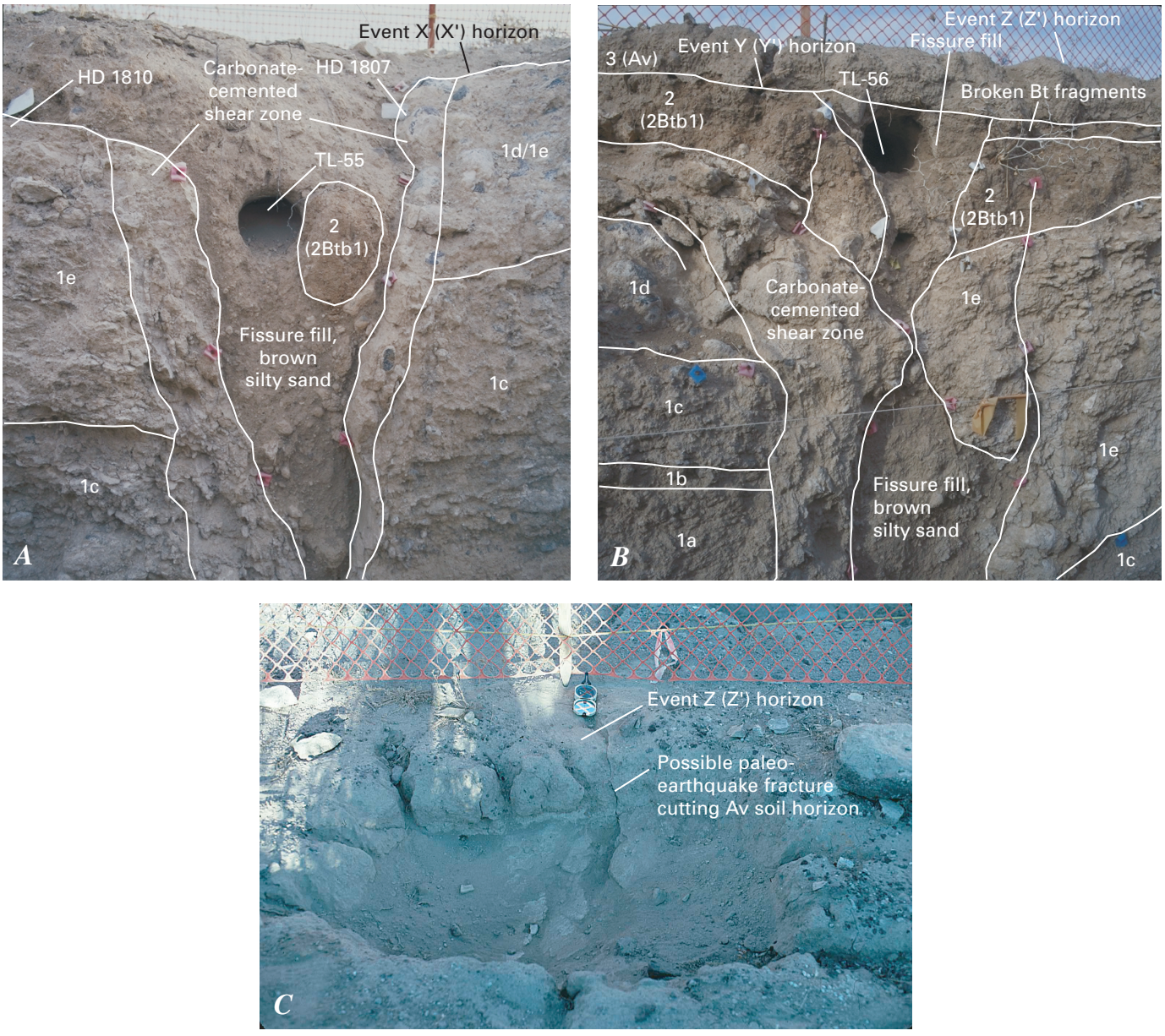

Figure 58. Parts of east and west walls of trench RV5 across southern strand of southern fault of the Rock Valley Fault system in Rock Valley, southwestern Nevada (pl. 25; figs. 1, 2, 51). *A*, Fault exposed in east wall. *B*, Fault exposed in west wall; Av soil horizon was stripped off during excavation. *C*, Possible paleoearthquake fracture extending to ground surface immediately west of west wall. Note compass for scale.

Table 42. Summary of faulting events on the Rock Valley Fault system in the Yucca Mountain area, southwestern Nevada.

[See figures 1, 2, and 51 for locations, and table 39 for estimated ages of samples. Fault displacements and event dates are best estimates. NA, not available]

Local event/ system-wide event	Likelihood of occurrence based on available evidence	Event horizon	Evidence	Vertical displacement	Net vertical displacement	Total net displacement	Estimated age
Northern fault of the Rock Valley Fault system—trenches RV3, RV3CT, and RV3A							
Z/Y'	Definite	Within Bkw soil horizon in trench RV3; at top of unit 6 in trench RV3A.	Fissure fill that terminates near base of A soil horizon in trenches RV3 and RV3CT; fractures that terminate at the base of unit 7b in trench RV3A; presence of a fining-upward sequence of colluvial-wedge deposits (units 7a–7d) in trench RV3A.	51 cm; (average of 63 cm measured as maximum height of unit 7 in trench RV3A, 84 cm measured at base of unit 5 in trench RV3CT, and 7 cm measured at base of unit 5 in trench RV3).	<51 cm, assuming minor back-rotation of downthrown block.	<267, cm calculated by using net vertical displacement and 11° rake. Cumulative net displacement for events Z–pre-W cannot exceed 14.3 m; therefore, 267 cm is considered a maximum.	13±4 ka; older than 11±2 ka (sample TL–58 from unit 8 in trench RV3A); probably younger than 12±5 ka (sample TL–57 from unit Bkw in trench RV3).
Y/X'	Moderate to high	Base of unit 4 in trenches RV3 and RV3CT and base of unit 5 in trench RV3A.	Wedge deposits. Unit 5 in trench RV3A and lower part of unit 4 in trench RV3.	69 cm; average of maximum thicknesses of 53 cm for unit 5 in trench RV3A, 109 cm for unit 4 in trench RV3, and 46 cm for unit 4 in trench RV3CT).	<69 cm, assuming minor back-rotation of downthrown block.	<362 cm, calculated by using estimated net vertical displacement and rake of 11°. Cumulative net displacement for events Z–pre-W cannot exceed 14.3 m; therefore, 362 cm is considered a maximum.	12–80 ka; older than 12±5 ka (sample TL–57); probably younger than approximately 80 ka (sample HD 1812).
X/W'	Moderate to high	Base of unit 3d in trenches RV3 and RV3CT.	Poorly defined wedge deposit (unit 3d) in trenches RV3 and RV3CT; subunits of unit 3 present on downthrown fault block, absent on upthrown block; displacement of unit 3b.	39 cm (maximum thickness of unit 3d in trench RV3).	<39 cm, assuming minor back-rotation of downthrown block.	<204 cm, calculated by using estimated average vertical tectonic displacement and rake of 11°. Cumulative net displacement for events Z–pre-W cannot exceed 14.3 m; therefore, 204 cm is considered a maximum.	About 120 ka; 80 to 300 ka, based solely on samples HD 1812 and HD 1954.
W/V'	Moderate to high	Base of unit 3b in trench RV3.	Poorly defined wedge deposit (unit 3b) in trench RV3.	63 cm (maximum thickness of unit 3b).	<63 cm, assuming minor back-rotation of downthrown block.	<330 cm, calculated by using estimated average vertical tectonic displacement and rake of 11°. Cumulative net displacement for events Z–pre-W cannot exceed 14.3 m; therefore, 330 cm is considered a maximum.	About 160 ka; 80 to 300 ka, based solely on samples HD 1812 and HD 1954.
Pre-W/ pre-V'	Low to moderate	Faulting events predating event V possibly occurred during deposition of unit 2a and before deposition of unit 3b in trench RV3, but little direct evidence exists on which to base reliable interpretations.	NA	NA	NA	NA	Older than 102–300 ka (samples HD 1955, HD 1954).
Medial fault of the Rock Valley Fault system—trenches RV1 and RV2 (Yount and others, 1987)							
Z/Z'	Poor to moderate	Top of Av soil horizon.	Possible fractures that cut Av soil horizon	If it occurred, probably 0–10 cm.	If it occurred, probably less than 10 cm.	If it occurred, probably less than 30 cm.	Younger than 7±1 ka (sample TL–75).
Y/Y'	Definite	Top of B soil horizon (unit C).	Multiple shear zones that terminate at top of B soil horizon. Vertical offset of B soil horizon.	<5–32 cm ----------	<32 cm, assuming minor back-rotation of downthrown block.	>32 cm, assuming oblique slip.	Older than 7±1 ka (sample TL–75); younger than 47±4 ka (sample TL–74).

Table 42. Summary of faulting events on the Rock Valley Fault system in the Yucca Mountain area, southwestern Nevada.—Continued

Local event/ system-wide event	Likelihood of occurrence based on available evidence	Event horizon	Evidence	Vertical displacement	Net vertical displacement	Total net displacement	Estimated age
Medial fault of the Rock Valley Fault system—trenches RV1 and RV2 (Yount and others, 1987)							
Pre-Y/Y'	Definite	Between the base of unit C and the top of unit E.	Differential offset of units C and E.	225–290 cm----------	<290 cm, assuming minor back-rotation of downthrown block.	>290 cm, assuming oblique slip.	Younger than 180 ka (Yount and others, 1987).
Northern strand of the Southern Rock Valley Fault system—trenches RV4 and RV4A							
Z/Z'	Definite	Top of Av soil horizon	Av soil horizon displaced; multiple fractures cutting Av soil horizon; wide disrupted zone in trench RV4A.	0–10 cm ----------	0–10 cm, measured at top of Av soil horizon.	Unknown, but probably at least 10 cm, assuming oblique slip.	Younger than 2.0±0.5 ka (sample TL–53).
Y/Y'	Moderate	Top of BW soil horizon (top of unit 4).	Silt fill in fault zone in trenches RV4 and RV4A is cut by fractures created by event Z; few poorly defined fractures appear to terminate within or at base of platy K soil horizon, which may be evidence for either this event or for next earlier event (X), or which may reflect both of these events.	0–10 cm ----------	0–10 cm	Unknown, but probably at least 10 cm, assuming oblique slip.	Older than 2±0.5 ka (sample TL–53); younger than 64±2 ka (sample HD 1804).
X/X'	Moderate	Top of unit 3	A few poorly defined fractures appear to terminate within or at base of platy K soil horizon, possibly reflecting either event Y or event X, or both; there is differential displacement of units 1–3 relative to unit 4.	0–10 cm ----------	0–10 cm	Unknown, but probably at least 10 cm, assuming oblique slip.	Older than 16.4±0.3 ka (sample HD 1805); younger than 64±2 ka (sample HD 1804).
Southern strand of the southern fault of the Rock Valley Fault system—trench RV5							
Z/Z'	Poor to moderate	Top of Av soil horizon.	Extension fractures cut Av soil horizon in trench RV 5 and in a shallow pit west of trench.	– –	– –	– –	Younger than 6±1 ka (sample TL–56).
Y/Y'	Definite	Top of Bt soil horizon (unit 2).	Silt-filled fissure containing pods of Bt soil-horizon material.	0–10 cm ----------	0–10 cm --------	0–34 cm, (computed using a 17° rake).	Older than 10±1 ka (sample TL–55); younger than 72±10 ka (sample HD 1807).
X/X'	High	Top of K soil horizon (unit 1).	Multiple fractures, which are differentiated from those of event Y by being engulfed by carbonate, terminate at or near top of K horizon; event probably occurred during carbonate soil formation.	2–22 cm ----------	2–22 cm --------	7–75 cm, (computed using a 17° rake).	Older than 10±5 ka (HD 1810); younger than 72±10 ka (sample HD 1807).
Trench in Frenchman Flat							
Z/Y'	Definite	Within B soil horizon (unit B).	Two shear zones that offset oldest part (Bw soil) of B soil horizon and form a graben.	As measured on west wall at base of unit B, 1.40 m down-to-the-north at the southern shear zone, 0.46 m down-to-the-south at the northern shear zone.	100±25 cm	>1.0±0.25 m, assuming oblique slip.	8–29 ka; older than 9±1 ka (sample TL–72); younger than 27±2 ka (sample TL–73).

ka. Therefore, for the purpose of determining recurrence intervals (see next section), we evenly distribute the faulting events within this time interval and estimate that event V′ occurred about 160 ka and event W′ about 120 ka. Total net displacement for event V′ was less than 330 cm down to the south, and slip for event W′ was less than 204 cm down to the south.

Slip Rates and Recurrence Intervals

Northern Fault

The total net cumulative displacement of unit 2a in trench RV3 (fig. 55) is about 14.3±2.8 m (pl. 23). Our best estimated age for unit 2a is 200±100 ka. Given these constraints and following the methods of McCalpin (1996, p. 457), we calculate the slip rate for the northern fault at 0.072±0.038 mm/yr.

At least four faulting events occurred between about 160 and 9 ka on the northern fault. Using the best estimated dates for these events (see preceding section), the best estimated recurrence intervals are about 27 k.y. (events Y′–X′), 80 k.y. (events X′–W′), and 40 k.y. (events W′–V′).

Medial Fault

The cumulative vertical offset of stratigraphic units reported by Yount and others (1987) on the medial fault in trench RV2 (fig. 51) is 2.57 to 2.95 m. Calculations using these values and a 22° rake from slickensides exposed in bedrock east of the trench indicate a net displacement ranging from 6.86 to 7.87 m. Yount and others (1987) reported U-trend ages of 180±40, 270±30, and 390±100 ka on three samples from one of the oldest displaced trench units that probably correlates with unit Qa2 and (or) unit Qa3 of the standard Yucca Mountain stratigraphic sequence (col. 1, table 2) and with unit Q2c of Swadley and others (1984) (col. 2, table 2). The U-trend ages, though considered to be generally unreliable (as discussed in chap. 2), fall in the middle to late Pleistocene, which is the time interval assigned to units Qa2–Qa3 and Q2c. The reported displacements and estimated age limits can therefore be expressed as 7.36±0.50 m and 315±140 ka, respectively, for calculating the slip rate according to the methods of McCalpin (1996), resulting in a slip rate of 0.023±0.010 mm/yr for the medial fault.

The best estimated dates for faulting events exposed in trenches on the medial fault are 13±4 ka for event Y′ and later than 180 ka for an earlier event(s), resulting in a single recurrence interval of about 170 k.y. Because the pre-event Y′ horizon is at the top of the K soil horizon, however, that event probably represents event X′, and so the recurrence interval between events Y′ and X′ on the medial fault is considered to be the same (27 k.y.) as that calculated for the other major faults in the Rock Valley Fault system.

Northern Strand of the Southern Fault

The cumulative vertical displacement of unit 2 in trench RV4 (fig. 51) is about 10±5 cm, but the net cumulative displacement could not be determined because no slip-direction indicators were observed in the trench. However, if we assume that the fault has oblique-slip movement—which is likely, considering the surface expression of the fault and the focal mechanisms of recent earthquakes in Rock Valley, as well as the 17° rake of slickensides observed in trench RV5 on the southern splay of the southern fault—then the minimum net cumulative displacement may be about 10±5 cm. The age of unit 2 was estimated at 88±74 ka by thermoluminescence analysis. Given these constraints and following the methods of McCalpin (1996), we calculate a minimum slip rate of 0.001±0.001 mm/yr.

Three faulting events have occurred on the northern splay of the southern fault in the past 40 k.y. Using the best estimated dates for these events, the recurrence intervals are about 9–10 k.y. (events Z′–Y′) and 27 k.y. (events Y′–X′).

Southern Strand of the Southern Fault

The cumulative vertical displacement of the top of unit 1 in trench RV5 is 12 to 22 cm down to the north (pl. 25). Using a displacement of 17±5 cm and a rake of 17° yields a cumulative net displacement of 58±17 cm. Unit 1 in trench RV5 is older than 320 ka. Given these constraints, the maximum slip rate for the southern splay of the southern fault is 0.002±0.0005 mm/yr.

Three faulting events have occurred on the southern splay of the southern fault in the past 40 k.y. Using the best estimated dates for these events, the recurrence intervals are about 9–10 k.y. (events Z′–Y′) and 27 k.y. (events Y′–X′).

Frenchman Flat Fault

The cumulative vertical displacement of the lower part of unit B (27±2 ka; sample TL–73, pl. 26; table 39) in the Frenchman Flat trench is about 1.0±0.25 m. No slickenlines were observed, and so the net cumulative displacement of unit B could not be determined; however, oblique-slip movement seems likely for the reasons already stated for other faults, and so 1.0±0.25 m should be considered the minimum net cumulative displacement. Because we observed evidence for only one surface-rupturing paleoearthquake (event Y′) in the trench, slip rates and recurrence intervals for the Frenchman Flat Fault could not be estimated.

Fault-System-Wide

The slip rate for the entire Rock Valley Fault system is estimated at 0.1 mm/yr by summing the estimated slip rates on the individual faults. The recurrence intervals for faulting events along one or more of these faults are about 9–10 k.y. (events Z′–Y′), 27 k.y. (events Y′–X′), 80 k.y. (events X′–W′), and 40 k.y. (events W′–V′).

Discussion

Low-angle striae and cumulative displacements of units in trenches indicate that Quaternary fault activity in central Rock Valley is predominantly transtensional—that is, the valley between the northern and southern faults, and particularly between the northern and medial faults, has been subsiding, and all the faults have a strong left-lateral-slip component. The striae range in rake from 11° to 22°, with a northeastward plunge on the down-to-the-south northern fault and a southwestward plunge on the down-to-the-north medial and southern faults. Fault-plane solutions from recent small earthquakes also indicate low-angle, left-lateral slip along near-vertical fault planes within the fault system.

The Quaternary slip rate of 0.1 mm/yr for the entire Rock Valley Fault system is close to the long-term (past 30 m.y.) slip rate of 0.089 mm/yr calculated by O'Leary (2000). This similarity indicates that slip along the fault system has remained relatively constant since middle Oligocene time.

At least two faulting events (X′, Y′) caused surface ruptures along two or more faults. Event X′ (40±24 ka) caused surface ruptures along the northern and southern faults, and, possibly, along the medial fault. Event Y′ (13±4 ka) caused surface displacement along all the faults in central Rock Valley, as well as along the Frenchman Flat Fault, indicating surface rupture over a distance of at least 23 km. The effect of event Y′ in western Rock Valley and Amargosa Valley is unknown. However, a recent study of scarps in Amargosa Valley along the possible southwestward extension of the Rock Valley Fault system indicates that the most recent faulting event was late Pleistocene (128–10 ka; Anderson and others, 1995). Therefore, event Y′ may have caused a surface rupture that extended from Frenchman Flat to Amargosa Valley (a distance of ~65 km).

Because of their close spacing (generally <2 km) and moderate to high degree of interconnectedness at the surface, individual faults within the Rock Valley Fault system probably would not extend as independent structures to seismogenic depths (typically ~15 km in the Great Basin). Therefore, we suspect that at least some (possibly most) of these faults merge at depth, and so an earthquake of a particular magnitude could cause surface ruptures along multiple faults in Rock Valley, as was especially evident during event Y′ in the past.

Acknowledgments

We thank Alan Ramelli, Jan Zigler, Michelle Murray, and Chris de Fontaine for their efforts in logging, describing, and interpreting the trenches. We also thank Jeff McCleary and Susan Olig for their field reviews of the logging and paleoseismic interpretations. We are grateful to Chris Menges for helping locate trenches RV3, RV4, and RV5 and for many helpful discussions and suggestions related to the calculation of moment magnitudes.